ACOUSTICS, SHALLOW WATER

F. B. Jensen, SACLANT Undersea Research Centre, La Spezia, Italy

doi:10.1006/rwos.2001.0313

Introduction

Using the commonly accepted definition of shallow water to mean coastal waters with depth up to 200 m, the shallow-water regions of the world constitute around 8% of all oceans and seas. These regions are particularly important since they are national economic zones and also more assessible.

Sound waves in the sea play the role of light in the atmosphere, i.e. acoustics is the only means of 'seeing' objects at distances beyond a few hundred meters in seawater. All forms of electromagnetic waves (light, radar) are rapidly attenuated in seawater. Low-frequency acoustic signals, on the other hand, propagate with little attenuation and can be heard over thousands of kilometers in the deep ocean.

The use of sound in the sea is ubiquitous. It is employed by the military to detect mines and submarines, and ship-mounted sonars measure water depth, ship speed and the presence of fish shoals. Side-scan systems are used to map bottom topography, sub-bottom profilers for getting information about the deeper layering, and other sonar systems for locating pipelines and cables on and beneath the seafloor. Sound is also used for navigating submerged vehicles, for underwater communications and for tracking marine mammals. In an inverse sense sound is used for measuring physical parameters of the ocean environment and for monitoring oceanic processes through the techniques of acoustical oceanography and ocean acoustic tomography.

Optimal sonar design for this great variety of applications demands using a wide range of acoustic frequencies. Practical shallow-water systems cover a frequency range from 50 Hz to 500 kHz, which, with a mean sound speed of 1500 m s^{-1}, correspond to acoustic wavelengths from 30 m down to 3 mm.

The principal characteristic of shallow-water propagation is that the sound-speed profile is nearly constant over depth or downward refracting, meaning that long-range propagation takes place exclusively via lossy bottom-interacting paths. This is very different from deep-water scenarios, where the sound-speed structure is such that sound is refracted away from the bottom and therefore can propagate to long ranges with little attenuation. Moreover, the environmental variability is much higher in coastal regions than in the deep ocean, with the result that there is much more acoustic variability in shallow water than in deep water.

The Ocean Acoustic Environment

The ocean is an acoustic waveguide limited above by the sea surface and below by the seafloor. The speed of sound in the waveguide plays the same role as the index of refraction does in optics. Sound speed is normally related to density and compressibility. In the ocean, density is related to static pressure, salinity and temperature. The sound speed in the ocean is an increasing function of temperature, salinity, and pressure, the latter being a function of depth. It is customary to express sound speed (c) as an empirical function of three independent variables: temperature (T) in degrees centigrade, salinity (S) in parts per thousand (‰), and depth (D) in meters. A simplified expression for this dependence is

$$c = 1449.2 + 4.6\,T - 0.055\,T^2 + 0.00029\,T^3 + (1.34 - 0.010\,T)(S - 35) + 0.016\,D \quad [1]$$

In shallow water, where the depth effect on sound speed is small, the primary contributor to sound speed variations is the temperature. Thus, for a salinity of 35‰, the sound speed in seawater varies between 1450 m s^{-1} at 0°C and 1545 m s^{-1} at 30°C.

Seasonal and diurnal changes affect the oceanographic parameters in the upper ocean. In addition, all of these parameters are a function of geography. In a warmer season (or warmer part of the day) in shallow seas where tidal mixing is weak, the temperature increases near the surface and hence the sound speed increases toward the sea surface. This near-surface heating (and subsequent cooling) has a profound effect on surface-ship sonars. Thus the diurnal heating causes poorer sonar performance in the afternoon – a phenomenon known as the afternoon effect. The seasonal variability, however, is much greater and therefore more important acoustically.

A ray picture of propagation in a 100-m deep shallow water duct is shown in **Figure 1**. The sound-speed profile in the upper panel is typical of the Mediterranean in the summer. There is a warm surface layer causing downward refraction and hence repeated bottom interaction for all ray paths. Since the seafloor is a lossy boundary, propagation

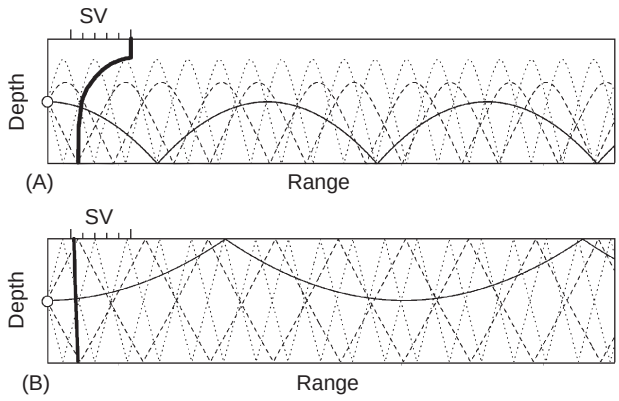

Figure 1 Ray paths in shallow water for typical Mediterranean summer and winter profiles. (A) In summer sound interacts repeatedly with the seabed but not with the sea surface. (B) In winter sound interacts with both the sea surface and the seabed, except for shallow rays emitted near the horizontal.

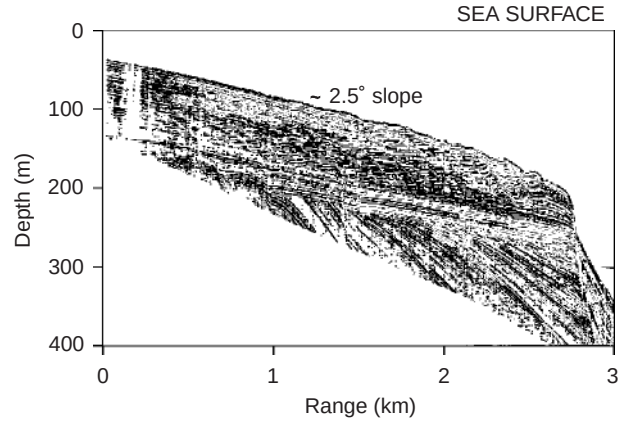

Figure 3 Seismic profile of bottom layering in coastal-water area of the Mediterranean.

in shallow water is dominated by bottom reflection loss at low and intermediate frequencies (< 1 kHz) and scattering losses at high frequencies. The seasonal variation in sound-speed structure is significant with winter conditions being nearly iso-speed (**Figure 1B**). The result is that there is less bottom interaction in winter than in summer, which again means that propagation conditions are generally better in winter than in summer.

Of course, the ocean sound-speed structure is neither frozen in time nor space. On the contrary, the ocean has its own weather system. There are currents, internal waves and thermal microstructure present in most shallow-water areas. **Figure 2** illustrates the sound speed variability along a 15 km-long track in the Mediterranean Sea. The data were recorded on a towed thermistor chain covering depths between 5 and 90 m. In general, this type of time-varying oceanographic structure has an effect on sound propagation, both as a source of attenuation (acoustic energy being scattered into steeper-angle propagation paths suffers increased bottom reflection loss) and of acoustic signal fluctuations with time.

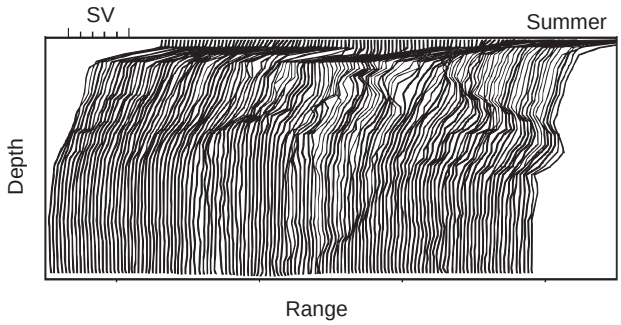

Figure 2 Spatial variability of sound speed in shallow-water area of the Mediterranean. The depth covered is around 100 m and the range 15 km.

Turning to the upper and lower boundaries of the ocean waveguide, the sea surface is a simple horizontal boundary and a nearly perfect reflector. The seafloor, on the other hand, is a lossy boundary with varying topography. Both boundaries have small-scale roughness associated with them which causes scattering and hence attenuation of sound due to the increased bottom reflection loss associated with steep-angle propagation paths. In terms of propagation physics, the seafloor is definitely the most complex boundary, exhibiting vastly different reflectivity characteristics in different geographical locations.

The structure of the ocean bottom in shallow water generally consists of a thin stratification of sediments overlying the continental crust. The nature of the stratification is dependent on many factors, including geological age and local geological activity. Thus, relatively recent sediments will be characterized by plane stratification parallel to the sea bed, whereas older sediments and sediments close to the crustal plate boundaries may have undergone significant deformation. An example of a complicated bottom layering is given in **Figure 3**, which displays a seismic section from the coastal Mediterranean. The upper stratification here is almost parallel to the seafloor, whereas deeper layers are strongly inclined.

Transmission Loss

The decibel (dB) is the dominant unit in ocean acoustics and denotes a ratio of intensities (not pressures) expressed on a $\log_{10}$ scale.

An acoustic signal traveling through the ocean becomes distorted due to multipath effects and

weakened due to various loss mechanisms. The standard measure in underwater acoustics of the change in signal strength with range is transmission loss defined as the ratio in decibels between the acoustic intensity $I(r,z)$ at a field point and the intensity I_0 at 1 m distance from the source, i.e.

$$\begin{aligned}\mathrm{TL} &= -10\log\frac{I(r,z)}{I_0}\\ &= -20\log\frac{|p(r,z)|}{|p_0|}\quad [\mathrm{dB\ re\ 1\,m}].\end{aligned}\qquad [2]$$

Here use has been made of the fact that the intensity of a plane wave is proportional to the square of the pressure amplitude. The major contributors to transmission loss in shallow water are: geometrical spreading loss, water volume attenuation, bottom reflection loss, and various scattering losses.

Geometrical Spreading

The spreading loss is simply a measure of the signal weakening as it propagates outward from the source. **Figure 4** shows the two geometries of importance in underwater acoustics. First consider a point source in an unbounded homogeneous medium (**Figure 4A**). For this simple case the power radiated by the source is equally distributed over the surface area of a sphere surrounding the source. If the medium is assumed to be lossless, the intensity is inversely proportional to the surface of the sphere, i.e. $I \propto 1/(4\pi R^2)$. Then from eqn [2] the spherical spreading loss is given by

$$\mathrm{TL} = 20\log r \quad [\mathrm{dB\ re\ 1\,m}] \qquad [3]$$

where r is the horizontal range in meters.

When the medium has plane upper and lower boundaries as in the waveguide case in **Figure 4B**, the farfield intensity change with horizontal range becomes inversely proportional to the surface of a cylinder of radius R and depth D, i.e. $I \propto 1/(2\pi RD)$. The cylindrical spreading loss is therefore given by

$$\mathrm{TL} = 10\log r \quad [\mathrm{dB\ re\ 1\,m}] \qquad [4]$$

Note that for a point source in a waveguide, there is spherical spreading in the nearfield ($r \leq D$) followed by a transition region toward cylindrical spreading which applies only at longer ranges ($r \gg D$).

As an example consider propagation in a shallow-water waveguide to a range of 20 km with spherical spreading applying on the first 100 m. The total propagation loss (neglecting attenuation) then becomes: 40 dB + 23 dB = 63 dB. This figure represents the minimum loss to be expected at 20 km. In practice, the total loss will be higher due both to the attenuation of sound in seawater, and to various reflection and scattering losses.

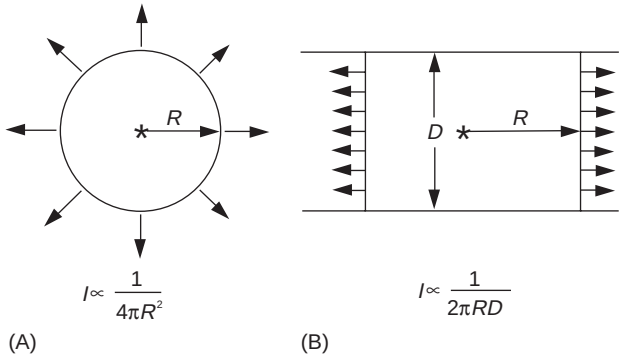

Figure 4 Geometrical spreading laws. (A) Spherical spreading; (B) Cylindrical spreading.

Sound Attenuation in Seawater

When sound propagates in the ocean, part of the acoustic energy is continuously absorbed, i.e. the energy is transformed into heat. Moreover, sound is scattered by different kinds of inhomogeneities, also resulting in a decay of sound intensity with range. As a rule, it is not possible in real ocean experiments to distinguish between absorption and scattering effects; they both contribute to sound attenuation in seawater.

A simplified expression for the frequency dependence (f in kHz) of the attenuation is given by Thorp's formula,

$$\alpha = \frac{0.11f^2}{1+f^2} + \frac{44f^2}{4100+f^2} \quad [\mathrm{dB\,km^{-1}}], \qquad [5]$$

where the two terms describe absorption due to chemical relaxations of boric acid, $B(OH)_3$, and magnesium sulphate, $MgSO_4$, respectively.

According to eqn [5] the attenuation of low-frequency sound in seawater is indeed very small. For instance, at 100 Hz a tenfold reduction in sound intensity (-10 dB) occurs over a distance of around 8300 km. Even though attenuation increases with frequency ($r_{-10\,\mathrm{dB}} \simeq 150$ km at 1 kHz and $\simeq 9$ km at 10 kHz), no other kind of radiation can compete with sound waves for long-range propagation in the ocean.

Bottom Reflection Loss

Reflectivity, the ratio of the amplitudes of a reflected plane wave to a plane wave incident on an interface separating two media, is an important measure of the effect of the bottom on sound propagation. Ocean bottom sediments are often modeled as fluids

which means that they support only one type of sound wave – a compressional wave.

The expression for reflectivity at an interface separating two homogeneous fluid media with density ρ_i and sound speed c_i, $i = 1, 2$, was first worked out by Rayleigh as

$$R(\theta_1) = \frac{(\rho_2/\rho_1)\sin\theta_1 - \sqrt{((c_1/c_2)^2 - \cos^2\theta_1)}}{(\rho_2/\rho_1)\sin\theta_1 + \sqrt{((c_1/c_2)^2 - \cos^2\theta_1)}} \quad [6]$$

where θ_1 denotes the grazing angle of the incident plane wave of unit amplitude.

The reflection coefficient has unit magnitude, meaning perfect reflection, when the numerator and denominator of eqn [6] are complex conjugates. This can only occur when the square root is purely imaginary, i.e. for $\cos\theta_1 > c_1/c_2$ (total internal reflection). The associated critical grazing angle below which there is perfect reflection is found to be

$$\theta_c = \arccos\left(\frac{c_1}{c_2}\right) \quad [7]$$

Note that a critical angle only exists when the sound speed of the second medium is higher than that of the first.

A closer look at eqn [6] shows that the reflection coefficient for lossless media is real for $\theta_1 > \theta_c$, which means that there is loss ($|R| = 1$) but no phase shift associated with the reflection process. On the other hand, for $\theta_1 < \theta_c$ we have perfect reflection ($|R| = 1$) but with an angle-dependent phase shift. In the general case of lossy media (c_i complex), the reflection coefficient is complex, and, consequently, there is both a loss and a phase shift associated with each reflection.

The critical-angle concept is very important for understanding the waveguide nature of shallow-water propagation. **Figure 5** shows bottom loss curves ($\mathrm{BL} = -10\log|R|^2$) for a few simple fluid bottoms with different compressional wave speeds (c_p), densities and attenuations. Note that for a lossy bottom we never get perfect reflection. However, there is in all cases an apparent critical angle ($\theta_c \simeq 33^\circ$ for $c_p = 1800\,\mathrm{m\,s^{-1}}$ in **Figure 5**), below which the reflection loss is much smaller than for supercritical incidence. With paths involving many bottom bounces such as in shallow-water propagation, bottom losses even as small as a few tenths of a decibel per bounce accumulate to significant total losses since the propagation path may involve many tens or even hundreds of bounces.

Real ocean bottoms are complex layered structures of spatially varying material composition. A geoacoustic model is defined as a model of the real seafloor with emphasis on measured, extrapolated, and predicted values of those material properties important for the modeling of sound transmission. In general, a geoacoustic model details the true thicknesses and properties of sediment and rock layers within the seabed to a depth termed the effective acoustic penetration depth. Thus, at high frequencies ($> 1\,\mathrm{kHz}$), details of the bottom composition are required only in the upper few meters of sediment, whereas at low frequencies ($< 100\,\mathrm{Hz}$) information must be provided on the whole sediment column and on properties of the underlying rocks.

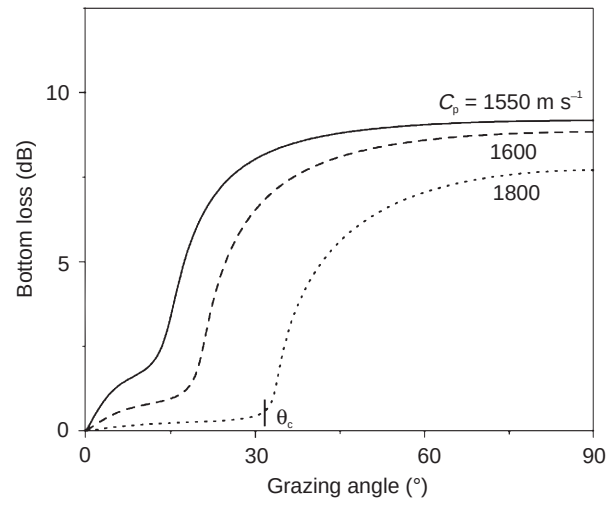

Figure 5 Bottom reflection loss curves for different bottom types. Note that low-speed bottoms (clay, silt) are more lossy than high-speed bottoms (sand, gravel). C_p is the compressional wave speed.

The information required for a complete geoacoustic model should include the following depth-dependent material properties: the compressional wave speed, c_p; the shear wave speed, c_s; the compressional wave attenuation, α_p; the shear wave attenuation, α_s; and the density, ρ. Moreover, information on the variation of all of these parameters with geographical position is required.

The amount of literature dealing with acoustic properties of seafloor materials is vast. **Table 1** lists the geoacoustic properties of some typical seafloor materials, as an indication of the many different types of materials encountered just in continental shelf and slope environments.

Boundary and Volume Scattering Losses

Scattering is a mechanism for loss, interference and fluctuation. A rough sea surface or seafloor causes attenuation of the mean acoustic field propagating in the ocean waveguide. The attenuation increases with increasing frequency. The field scattered away

Table 1 Geoacoustic properties of continental shelf environments

Bottom type	*p* (%)	ρ_b/ρ_w –	c_p/c_w –	c_p ($m\,s^{-1}$)	c_s ($m\,s^{-1}$)	α_p ($dB\,\lambda_p^{-1}$)	α_s ($dB\,\lambda_s^{-1}$)
Clay	70	1.5	1.00	1500	< 100	0.2	1.0
Silt	55	1.7	1.05	1575	c_s[a]	1.0	1.5
Sand	45	1.9	1.1	1650	c_s[b]	0.8	2.5
Gravel	35	2.0	1.2	1800	c_s[c]	0.6	1.5
Moraine	25	2.1	1.3	1950	600	0.4	1.0
Chalk	–	2.2	1.6	2400	1000	0.2	0.5
Limestone	–	2.4	2.0	3000	1500	0.1	0.2
Basalt	–	2.7	3.5	5250	2500	0.1	0.2

[a] $c_s = 80\,\tilde{z}^{0.3}$
[b] $c_s = 110\,\tilde{z}^{0.3}$
[c] $c_s = 180\,\tilde{z}^{0.3}$
$c_w = 1500\,\mathrm{m\,s^{-1}}$, $\rho_w = 1000\,\mathrm{kg\,m^{-3}}$.

from the specular direction, and, in particular, the backscattered field (called reverberation) acts as interference for active sonar systems. Because the ocean surface moves, it will also generate acoustic fluctuations. Bottom roughness can also generate fluctuations when the sound source or receiver is moving. The importance of boundary roughness depends on the sound-speed profile which determines the degree of interaction of sound with the rough boundaries.

Often the effect of scattering from a rough surface is thought of as simply an additional loss to the specularly reflected (coherent) component resulting from the scattering of energy away from the specular direction. If the ocean bottom or surface can be modeled as a randomly rough surface, and if the roughness is small with respect to the acoustic wavelength, the reflection loss can be considered to be modified in a simple fashion by the scattering process. A formula often used to describe reflectivity from a rough boundary is:

$$R'(\theta) = R(\theta)e^{-0.5\Gamma^2} \qquad [8]$$

where $R'(\theta)$ is the new reflection coefficient, reduced because of scattering at the randomly rough interface. Γ is the Rayleigh roughness parameter defined as

$$\Gamma \equiv 2k\sigma \sin\theta \qquad [9]$$

where $k = 2\pi/\lambda$ is the acoustic wavenumber and σ is the *rms* roughness. Note that the reflection coefficient for the smooth ocean surface is simply -1 (the pressure-release condition is obtained from eqn [6] by setting $\rho_2 = 0$) so that the rough-sea-surface reflection coefficient for the coherent field is $R'(\theta) = -\exp(-0.5\Gamma^2)$. For the ocean bottom, the appropriate geoacoustic parameters (see **Table 1**) are used for evaluating $R(\theta)$, and the rough-bottom reflection coefficient is then obtained from eqn [8].

Volume scattering is thought to arise primarily from biological organisms. For lower frequencies (less than 10 kHz), fish with air-filled swim bladders are the main scatterers whereas above 20 kHz, zooplankton or smaller animals that feed on the phytoplankton, and the associated biological food chain, are the scatterers. Many of the organisms undergo a diurnal migration rising towards the sea surface at sunset and descending to depth at sunrise. Since the composition and density of the populations vary with the environmental conditions, the scattering characteristics depend on geographical location, time of day, season and frequency. As an example, data from the Mediterranean Sea for volume scattering losses due to fish shoals show excess losses of 10–15 dB for a propagation range of 12 km and frequencies between 1 and 3 kHz.

Finally, scattering off bubbles near the surface is sometimes referred to as either a volume- or surface-scattering mechanism. These bubbles arise not only from sea surface action, but also from biological origins and from ship wakes. Furthermore, bubbles are not the only scattering mechanism, but bubble clouds may have significantly different sound speed than plain seawater thereby altering local refraction conditions. At the sea surface, the relative importance of roughness versus bubble effects is not yet resolved.

Transmission-loss Data

Figure 6 gives an example of transmission-loss variability in shallow water. The graph displays a collection of experimental data from different shallow-water areas (100–200 m deep) all over the world. The data refer to downward-refracting

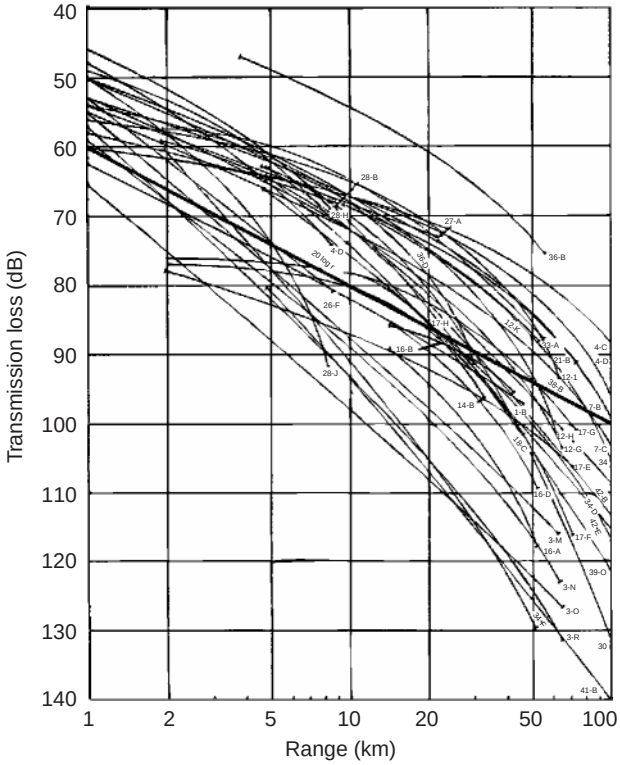

Figure 6 Transmission loss variability in shallow water.

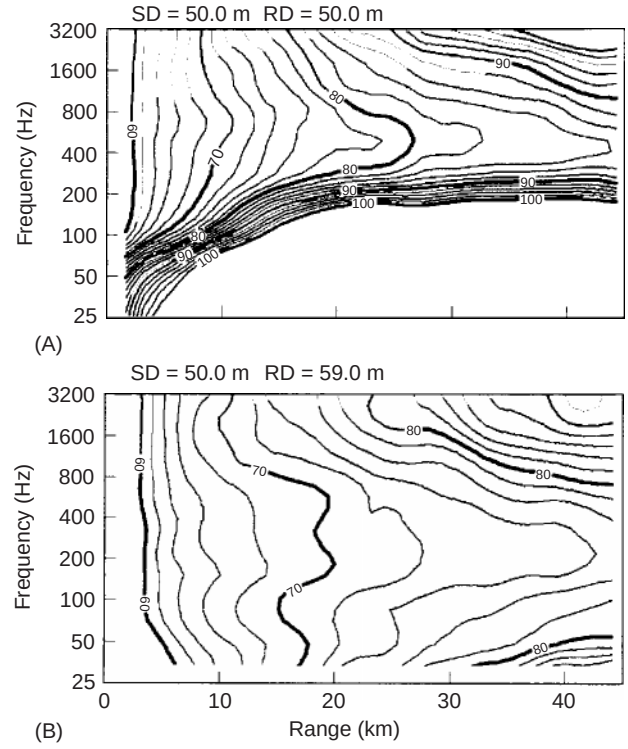

Figure 7 Examples of frequency-dependent propagation losses measured in two shallow-water areas: (A) Barents Sea, (B) English Channel. Note the presence of an optimum frequency of propagation between 200 and 400 Hz.

summer conditions in the frequency band 0.5–1.5 kHz. Two features are of immediate interest. One is the spread of the data amounting to around 50 dB at 100 km and caused primarily by the varying bottom-loss conditions in different areas of the world. The second feature is the fact that transmission is generally better than free-field propagation ($20 \log r$) at short and intermediate ranges but worse at longer ranges. This peculiarity is due to the trapping of energy in the shallow-water duct, which improves transmission at shorter ranges (cylindrical versus spherical spreading), but, at the same time, causes increased boundary interaction, which degrades transmission at longer ranges.

A second example of transmission-loss variability in shallow water is given in **Figure 7**, where broadband data from two different geographical areas are compared. The data set in **Figure 7A**, was collected in the Barents Sea in 60 m water depth. Note the high transmission losses recorded below 200 Hz, where energy levels fall off rapidly indicating that most of the acoustic energy emitted by the source is lost to the seabed. It is believed that this excess attenuation is caused by the coupling of acoustic energy into shear waves in the seabed. In contrast to the high-loss environment in the Barents Sea, **Figure 7B** shows a data set from the English Channel in 90 m water depth. Here propagation conditions are excellent over the entire frequency band. This second data set represents typical propagation conditions for thick sandy sediments with negligible shear-wave effects.

Cutoff Frequency and Optimum Frequency

A common feature of all acoustic ducts is the existence of a low-frequency cutoff. Hence, there is a critical frequency below which the shallow-water channel ceases to act as a waveguide, causing energy radiated by the source to propagate directly into the bottom. The cutoff frequency is given by,

$$f_0 = \frac{c_w}{4D\sqrt{(1 - (c_w/c_b)^2)}} \qquad [10]$$

This expression is exact only for a homogeneous water column of depth D and sound speed c_w overlying a homogeneous bottom of sound speed c_b. As an example, let us take $D = 100\,\text{m}$, $c_w = 1500\,\text{m s}^{-1}$, and $c_b = 1600\,\text{m s}^{-1}$ (sand–silt), which yields $f_0 \simeq 11\,\text{Hz}$.

Sound transmission in shallow water has the characteristic frequency-dependent behavior shown in **Figure 7**, i.e. there is an optimum frequency of propagation at longer ranges. Thus the 80 dB

contour line extends farthest in range for frequencies around 400 Hz in **Figure 7A** and around 200 Hz in **Figure 7B**, implying that transmission is best at these frequencies – the optimum frequencies of propagation for the two sites.

Optimum frequency is a general feature of ducted propagation in the ocean. It occurs as a result of competing propagation and attenuation mechanisms at high and low frequencies. In the high-frequency regime we have increasing volume and scattering loss with increasing frequency. At lower frequencies the efficiency of the duct to confine sound decreases (the cutoff phenomenon). Hence propagation and attenuation mechanisms outside the duct (in the seabed) become important. In fact, the increased penetration of sound into a lossy seabed with decreasing frequency causes the overall attenuation of waterborne sound to increase with decreasing frequency. Thus we get high attenuation at both high and low frequencies, whereas intermediate frequencies have the lowest attenuation. It can be shown that the optimum frequency for shallow-water propagation is strongly dependent on water depth ($f_{\text{opt}} \propto D^{-1}$), has some dependence on the sound-speed profile, but is only weakly dependent on the bottom type. Typically, the optimum frequency is in the range 200–800 Hz for a water depth of 100 m.

Signal Transmission in the Time Domain

Even though underwater acousticians have traditionally favored spectral analysis techniques for gaining information about the band-averaged energy distribution within a shallow-water waveguide, additional insight into the complication of multipath propagation can be obtained by looking at signal transmission in the time domain.

Figure 8 indicates that the signal structure measured downrange will consist of a number of arrivals with time delays determined by the pathlength differences, and individual pulse shapes being modified due to frequency-dependent amplitude and phase changes associated with each boundary reflection. From simple geometrical considerations, the time dispersion is found to be

$$\Delta_\tau \simeq \frac{R}{\bar{c}}\left(\frac{1}{\cos\theta} - 1\right) \qquad [11]$$

where R is the range between source and receiver, $\bar{c}$ is the mean sound speed in the channel, and θ is the maximum propagation angle with respect to the horizontal. This angle will be determined either by the source beamwidth or by the critical angle at the bottom (the smaller of the two). Since the dispersion considered here is solely due to the geometry of the waveguide, it is called geometrical dispersion.

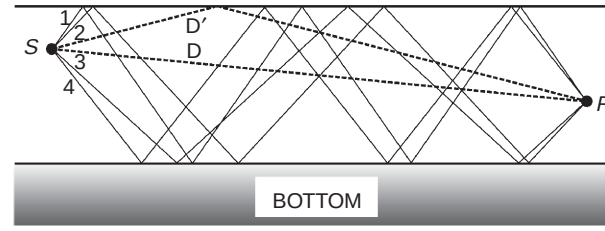

Figure 8 Schematic of ray arrivals in shallow-water waveguide. A series of multipath arrivals are expected, represented by eigenrays connecting source (S) and receiver (R). The shortest path is the direct arrival D followed by the surface-reflected arrival D'. Next comes a series of four arrivals all with a single bottom bounce; then four rays with two bottom bounces as illustrated in the figure, followed by four rays with three bottom bounces, etc.

An example of measured pulse arrivals over a 10 h period in the Mediterranean is given in **Figure 9**. Note that the time-varying ocean (internal waves, currents, tides) causes strong signal fluctuations with time, particularly in the earlier part of the signal. The time dispersion is 15–20 ms and at least four main energy packets, each consisting of several ray arrivals can be identified.

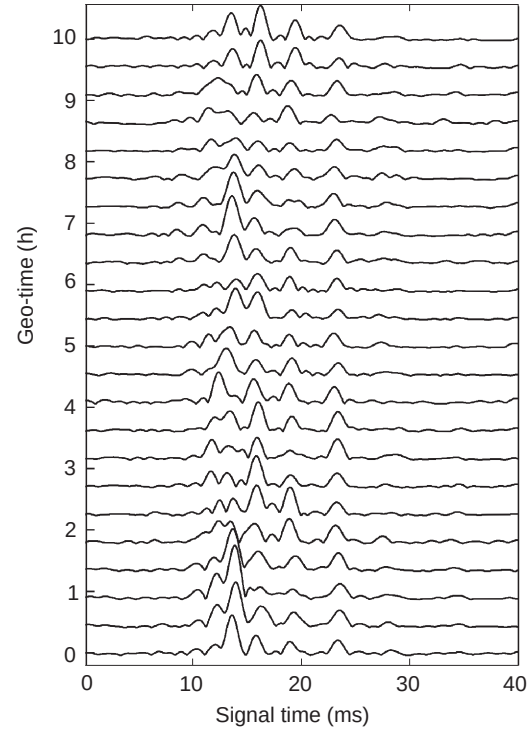

Figure 9 Measured pulse arrivals versus geo-time over a 10 km shallow-water propagation track in the Mediterranean Sea. The water depth is 130 m, the bandwidth is 200–800 Hz.

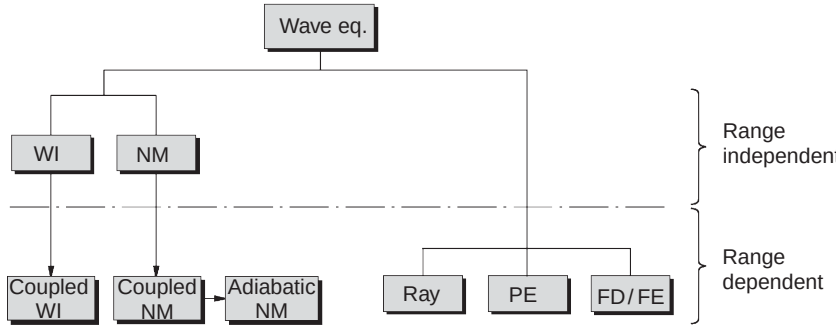

Figure 10 Hierarchy of numerical models in underwater acoustics. WI, wavenumber integration; NM, normal modes; PE, parabolic equation; FD, finite difference; FE, finite element.

Numerical Modeling

The advent of computers has resulted in an explosive growth in the development and use of numerical models since the mid-1970s. Numerical models have become standard research tools in acoustic laboratories, and computational acoustics is becoming an evermore important branch of the ocean acoustic science. Only the numerical approach permits an analysis of the full complexity of the acoustic problem.

An assortment of models has been developed over the past 25 years to compute the acoustic field in shallow-water environments in both the frequency and time domains. Entire textbooks are dedicated to the development of theoretical and numerical formalisms which can provide quantitative acoustic predictions for arbitrary ocean environments. Sound propagation is mathematically described by the wave equation, whose parameters and boundary conditions are descriptive of the ocean environment. As shown in **Figure 10**, there are essentially five types of models (computer solutions to the wave equation) to describe sound propagation in the sea: wavenumber integration (WI); normal mode (NM); ray; parabolic equation (PE) and direct finite-difference (FD) or finite-element (FE) solutions of the full wave equation. All of these models permit the ocean environment to vary with depth. A model that also permits horizontal variations in the environment, i.e. sloping bottom or spatially varying oceanography, is termed range dependent.

As shown in **Figure 10**, an *a priori* assumption about the environment being range independent, leads to solutions based on spectral techniques (WI) or normal modes (NM); both of these techniques can, however, be extended to treat range dependence. Ray, PE and FD/FE solutions are applied directly to range-varying environments. For high frequencies (a few kilohertz or above), ray theory, the infinite frequency approximation, is still the most practical, whereas the other five model types become more and more applicable below, say, a kilohertz in shallow water. Models that handle ocean variability in three spatial dimensions have also been developed, but these models are used less frequently than two-dimensional versions because of the computational cost involved.

Conclusions

The acoustics of shallow water has been thoroughly studied both experimentally and theoretically since World War II. Today the propagation physics is well understood and sophisticated numerical models permit accurate simulations of all processes (reflection, refraction, scattering) that contribute to the complexity of the shallow-water problem. Sonar performance predictability, however, is limited by knowledge of the controlling environmental inputs. The current challenge is therefore how best to collect relevant environmental data from the world's enormously variable shallow-water areas.

See also

Acoustics, Arctic. Acoustics, Deep Ocean. Acoustics in Marine Sediments. Acoustic Noise. Acoustic Scattering by Marine Organisms. Sonar Systems. Surface, Gravity and Capillary Waves. Tomography.

Further Reading

Brekhovskikh LM and Lysanov YP (1990) *Fundamentals of Ocean Acoustics*, 2nd edn. New York: Springer-Verlag.

Etter PC (1996) *Underwater Acoustic Modeling*, 2nd edn. London: E & FN Spon.

Jensen FB, Kuperman WA, Porter MB and Schmidt H (2000) *Computational Ocean Acoustics*. New York: Springer-Verlag.

Medwin H and Clay CS (1998) *Fundamentals of Acoustical Oceanography*. San Diego: Academic Press.

Urick RJ (1996) *Principles of Underwater Sound*, 3rd edn. Los Altos: Peninsula Publishing.